Children with severe asthma have substantial structural airway changes on computed tomography

Wytse B. van den Bosch [1,2], Qianting Lv[1,2], Eleni-Rosalina Andrinopoulou[3,4], Mariëlle W.H. Pijnenburg[1], Pierluigi Ciet [1,2,5], Hettie M. Janssens[1] and Harm A.W.M. Tiddens [1,2,6]

[1]Erasmus MC – Sophia Children's Hospital, University Medical Center Rotterdam, Department of Paediatrics, division of Respiratory Medicine and Allergology, Rotterdam, the Netherlands. [2]Erasmus MC, University Medical Center Rotterdam, Department of Radiology and Nuclear Medicine, Rotterdam, the Netherlands. [3]Erasmus MC, University Medical Center Rotterdam, Department of Biostatistics, Rotterdam, the Netherlands. [4]Erasmus MC, University Medical Center Rotterdam, Department of Epidemiology, Rotterdam, the Netherlands. [5]Department of Radiology, Policlinico Universitario, University of Cagliari, Cagliari, Italy. [6]Thirona BV, Nijmegen, the Netherlands.

Corresponding author: Harm A.W.M. Tiddens (h.tiddens@erasmusmc.nl)

Shareable abstract (@ERSpublications)
Is it time to rethink the role of imaging in severe asthma? Automatic bronchus–artery analysis and manual semiquantitative scoring of CTs from children with SA show substantial structural abnormalities, especially bronchiectasis and bronchial wall thickening. https://bit.ly/3qMKePC

Cite this article as: van den Bosch WB, Lv Q, Andrinopoulou E-R, *et al*. Children with severe asthma have substantial structural airway changes on computed tomography. *ERJ Open Res* 2024; 10: 00121-2023 [DOI: 10.1183/23120541.00121-2023].

This article has an editorial commentary: https://doi.org/10.1183/23120541.00763-2023

Received: 24 Feb 2023
Accepted: 17 Aug 2023

Abstract

Background In adults with severe asthma (SA) bronchial wall thickening, bronchiectasis and low attenuation regions (LAR) have been described on chest computed tomography (CT) scans. The extent to which these structural abnormalities are present in children with SA is largely unknown. Our aim was to study the presence and extent of airway abnormalities on chest CT of children with SA.

Methods 161 inspiratory and expiratory CT scans, either spirometer-controlled or technician-controlled, obtained in 131 children with SA (mean±SD age 11.0±3.8 years) were collected retrospectively. Inspiratory scans were analysed manually using a semi-quantitative score and automatically using LungQ (v2.1.0.1; Thirona B.V., Nijmegen, the Netherlands). LungQ segments the bronchial tree, identifies the generation for each bronchus–artery (BA) pair and measures the following BA dimensions: outer bronchial wall diameter (B_{out}), adjacent artery diameter (A) and bronchial wall thickness (B_{wt}). Bronchiectasis was defined as $B_{out}/A \geqslant 1.1$, bronchial wall thickening as $B_{wt}/A \geqslant 0.14$. LAR, reflecting small airways disease (SAD), was measured automatically on inspiratory and expiratory scans and manually on expiratory scans. Functional SAD was defined as $FEF_{25–75}$ and/or FEF_{75} z-scores <−1.645. Results are shown as median and interquartile range.

Results Bronchiectasis was present on 95.8% and bronchial wall thickening on all CTs using the automated method. Bronchiectasis was present on 28% and bronchial wall thickening on 88.8% of the CTs using the manual semi-quantitative analysis. The percentage of BA pairs defined as bronchiectasis was 24.62% (12.7–39.3%) and bronchial wall thickening was 41.7% (24.0–79.8%) per CT using the automated method. LAR was observed on all CTs using the automatic analysis and on 82.9% using the manual semi-quantitative analysis. Patients with LAR or functional SAD had more thickened bronchi than patients without.

Conclusion Despite a large discrepancy between the automated and the manual semi-quantitative analysis, bronchiectasis and bronchial wall thickening are present on most CT scans of children with SA. SAD is related to bronchial wall thickening.

Introduction

Severe asthma (SA) is an umbrella term for a heterogeneous disease that is characterised by ongoing asthma symptoms despite the use of high-dose inhaled medication and optimisation of modifiable factors such as poor adherence, poor inhaler technique and exposure to triggers [1]. Apart from inflammation,

bronchial hyperresponsiveness and increased mucus production, structural bronchial abnormalities are thought to play an important role in SA pathophysiology [2]. In pathology and imaging studies in adults with mild to severe asthma, structural bronchial changes have been observed in the larger central bronchi [3–6]. Besides larger bronchial changes, small airway changes or small airways disease (SAD) has also been described [7]. SAD has even been suggested to delineate a distinct phenotype of asthma called: "small airways phenotype" [8]. Structural airway changes in adults with SA could originate early in the course of the disease as biopsy studies in children show that structural changes are already present in preschool wheezers who later develop asthma [9–11].

Chest computed tomography (CT) is the gold standard for non-invasive *in vivo* assessment of structural bronchial and parenchymal changes in lung disease [12]. As chest CT is not standard of care in SA [13], there are only a few small observational studies that report findings on chest CTs of children with SA. In these studies, bronchial wall thickening, bronchiectasis, mucus plugging, ground glass opacities, consolidation, linear densities and low attenuation regions (LAR) (often described as "trapped air") were reported [11, 14–18]. In comparison to adults, children with SA seem to have less severe structural abnormalities. Importantly, it is unclear at what age these "early" structural abnormalities develop in children with SA and whether they progress into more severe and irreversible structural changes in adult life.

Sensitive techniques are needed to detect and quantify early structural abnormalities on chest CT in children with SA. In cystic fibrosis (CF) manual measurement of bronchial dimensions on chest CT has been shown to be a sensitive method to detect structural bronchial changes, such as subtle bronchial wall thickening and bronchial widening [19]. However, measuring all visible bronchi is a tedious task and therefore not routinely performed in current clinical practice. Currently, artificial intelligence is being used to develop automatic methods that can sensitively assess bronchial dimensions and parenchymal abnormalities on chest CT scans [20, 21]. Recently, an automatic method was developed to assess bronchial dimensions of all visible bronchus–artery (BA) pairs on an inspiratory chest CT scan. In CF patients this automatic BA analysis has been shown to be sensitive to detect bronchial wall thickening and bronchial widening [22, 23]. Furthermore, an automatic method was developed that is able to detect SAD by measuring differences in lung density between inspiratory and expiratory CT scans.

We aimed to study the presence and extent of the structural large and small bronchial abnormalities on chest CT scans of children with SA using a fully automatic system to measure bronchial dimensions and a manual semi-quantitative method to score other relevant structural changes. Furthermore, we aimed to assess the relation between structural abnormalities and multiple outcome measures of SAD. We hypothesised that substantial structural bronchial abnormalities are present in children with SA.

Methods

Study design

In this investigator-initiated observational study, we retrospectively collected chest CT scans from children with SA that underwent CT between 2007 and 2019 at the specialised asthma clinic of the Erasmus MC Sophia Children's Hospital (Rotterdam). Inspiratory and expiratory chest CT scans are performed routinely in many of our SA patients to rule out possible underlying conditions contributing to SA. Inclusion criteria were: age 4–18 years at time of CT and diagnosis of SA according to the Global Initiative for Asthma confirmed by the treating physician [24], and CTs with a slice thickness smaller than 1.5 mm as required for the automatic analysis. Exclusion criteria were: known pulmonary, thoracic or cardiac abnormality prior to CT and active smoking at the time of CT. The local medical ethics review committee reviewed the research protocol (MEC-2019–0554) and provided a waiver [25]. Informed consent was obtained before data collection was initiated.

Objectives and outcomes

To investigate the presence and extent of structural bronchial changes on CT in children with SA we used a fully automatic method to measure bronchial dimensions and LAR. In addition, we used a manual semi-quantitative scoring method to quantify structural bronchial changes and LAR. Furthermore, we investigated whether BA dimensions were associated with LAR and with functional indicators of SAD, such as forced expiratory flows between 25% and 75% of forced vital capacity ($FEF_{25–75}$) and at 75% (FEF_{75}) of forced vital capacity (FVC) measured by spirometry.

Clinical data collection

Patient records were reviewed for: asthma diagnosis, age at time of chest CT, height, weight, ever allergic sensitisation to aeroallergens, comorbidities, medication use and spirometry results. Forced expiratory

volume in 1 s (FEV_1), $FEF_{25–75}$ and FEF_{75} parameters are presented as per cent predicted values and z-scores according to the formulas reported by the Global Lung Function Initiative (GLI) [26]. All data were pseudonymised to ensure blinding for the image analysis.

Computed tomography

A list of all chest CT scans performed at our clinic was generated by searching the picture archiving and communication system for "asthma" and "CT" (figure 1). After this search, we excluded patients without a chest CT, patients that did not meet the criteria for SA, duplicate CT records and patients that met the exclusion criteria. For selected CT scans, we categorised the technique used to optimise lung volume during CT acquisition into 1) instructions given by a CT/lung function technician or 2) by a lung function technician with a CT compatible spirometer. The presence of a lung function technician during the CT and the use of a spirometer are routine care in our clinic to optimise inhalation (near total lung volume) and exhalation (near residual volume) during scanning [27].

Image analysis

Automatic bronchus–artery analysis

For the automatic analyses only CT scans with a slice thickness <1.5 mm were included. To measure BA dimensions on inspiratory scans we used automatic artificial intelligence (AI)-based software (LungQ-BA v2.1-rc; Thirona B.V., Nijmegen, the Netherlands) [22, 23]. LungQ software is trained with a large variety

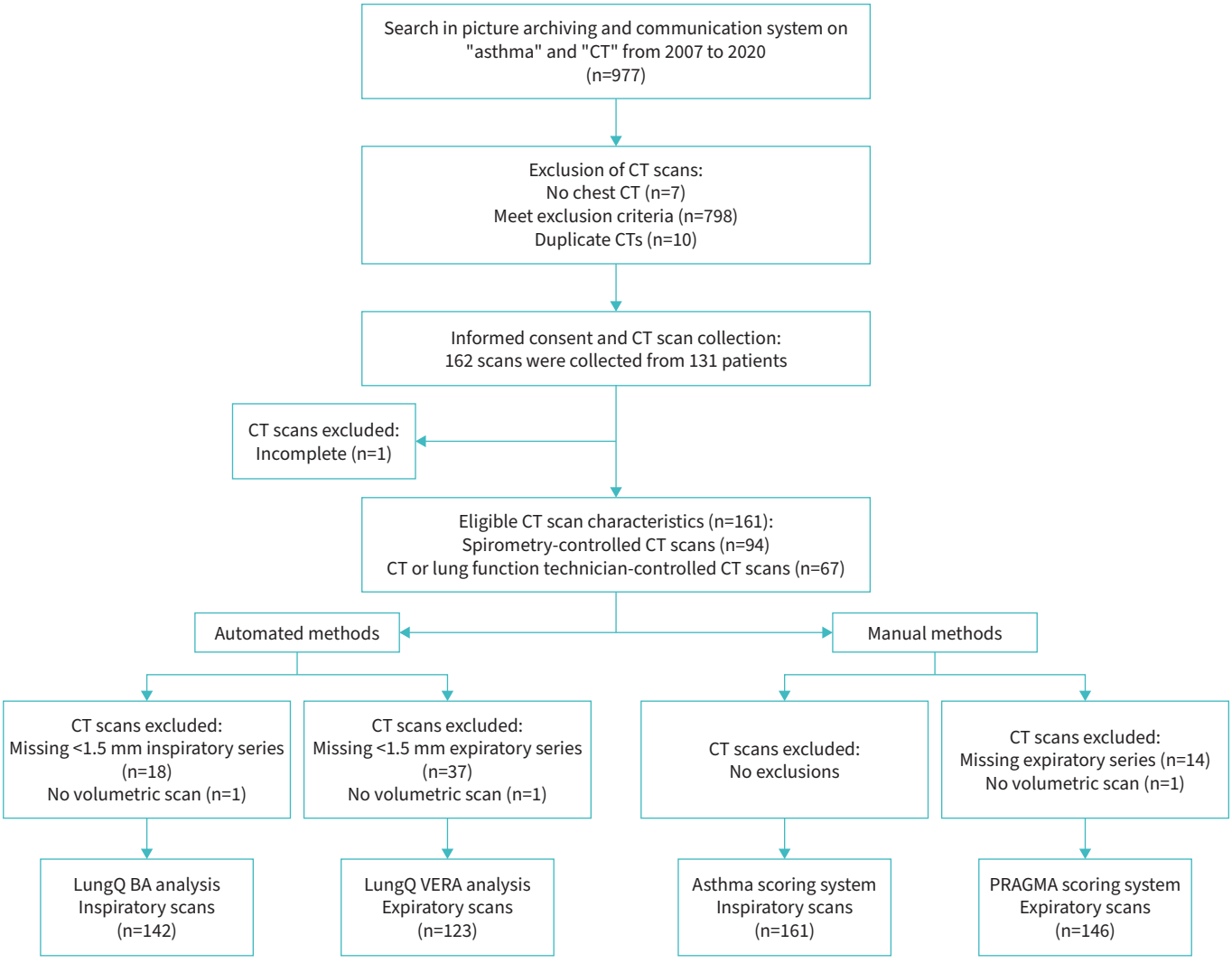

FIGURE 1 Flowchart of the eligible scans used for the different analysis methods. CT: computed tomography; BA: bronchus–artery.

of datasets of inspiratory and expiratory CTs to ensure robust performance against variation in patient characteristics (age, gender, body mass index), variation in disease populations (COPD, asthma, CF, interstitial lung disease, chronic bronchitis, bronchiectasis, COVID-19) and variation in image characteristics (manufacturer, dose, convolutional kernel, voxel spacing). This software first segments the entire bronchial tree. Next, it identifies for all bronchi their generations and adjacent arteries starting at the segmental level (G_0). The algorithm automatically measures for every bronchus the outer bronchial wall diameter (B_{out}), the bronchial lumen diameter (B_{lumen}), bronchial wall thickness (B_{wt}) and adjacent artery diameter (A) (figure 2). For every BA pair B_{out}/A and B_{lumen}/A were computed to define bronchiectasis, and B_{wt}/A to define bronchial wall thickening. Based on previous studies, we used a cut-off value of 1.1 for the B_{out}/A ($B_{out}A$) to define bronchiectasis [19, 22, 28, 29]. In addition, we also used a cut-off value of ⩾1.5 which has been proposed to define bronchiectasis in adults [28]. Bronchial wall thickening was defined as: B_{wt}/A ($B_{wt}A$) of ⩾0.14 and ⩾0.20 [22, 30]. For bronchial wall thickening we also included the ratio between bronchial wall area and bronchial outer area (B_{wa}/B_{oa}), which provides information on the degree of bronchial remodelling independent of artery diameter changes.

For the automatic quantification of SAD we used an AI-based method called: "Ventilation Estimation deep learning Analysis" (VERA) (LungQ). VERA is an artificial intelligence-based algorithm that utilises voxel-wise inspiratory–expiratory image registration and global lobar volume changes to classify and quantify regions with disproportionally low lung density changes. VERA provides a 3D heat map allowing to visualise the abnormal regions on top of the inspiratory CT scan; an example of this can be found in the supplementary figure S1. For this study we defined regions that showed disproportionally low lung density changes as SAD.

In addition, the LungQ software was used to segment and compute inspiratory and expiratory lung volume (in millilitres). We considered the volume on the inspiratory scan to be similar to the total lung capacity (TLC) and the volume on the expiratory scan to be similar to the residual volume (RV). We calculated the vital capacity (VC) by subtracting RV from TLC (VC=TLC – RV). Predicted values for TLC, RV and VC were computed using the GLI formulas [26].

Manual semi-quantitative scoring methods (asthma-CT)

Inspiratory scans were analysed using the "asthma-CT" scoring method. This semi-quantitative scoring method was adapted from the CF-CT scoring method [31], which is a well-standardised scoring method to assess structural lung abnormalities in patients with CF [31]. For scoring we used the thinnest slice available with a lung reconstruction kernel. Hereafter, we divided the lung into six lobes: left upper, lingula, left lower, right upper, right middle and right lower lobe. Secondly, for every lobe we evaluated whether bronchiectasis, bronchial wall thickening, mucus plugging, atelectasis/consolidation, bulla/cysts and/or ground glass opacities were present. Finally, the extent of bronchiectasis, bronchial wall thickening and mucus plugging within a lobe was scored; 1 = <33% of the lobe, 2 = 33% to 67% of the lobe and 3 = >67% of the lobe [31]. Total scores were calculated individually by adding up the sub scores of the six lobes (maximal score was 18).

For quantification of LAR only we used the well-established manual grid-based morphometric quantitative Perth–Rotterdam Annotated Grid Morphometric Analysis for CF (PRAGMA-CF) scoring method [32]. All grid cells that contain at least 50% of the lung field are annotated. Each grid cell that contains >50% of LAR is annotated accordingly [32]. The volume percentage of LAR (%LAR) is calculated by dividing the

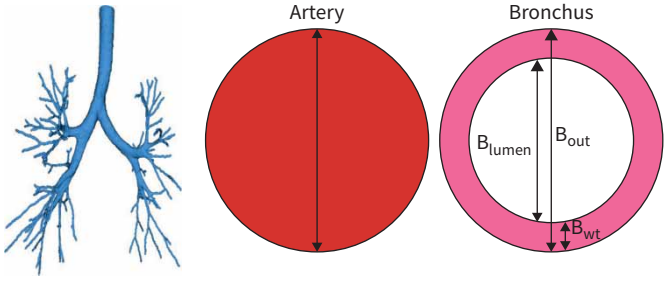

FIGURE 2 Example of an automatic bronchial tree segmentation by LungQ-BA software (Thirona B.V.) on the left, and a graphical display of the executed measurements of bronchus and adjacent artery dimensions on the right. B_{lumen}: bronchial lumen diameter; B_{out}: bronchial outer diameter; B_{wt}: bronchial wall thickness.

number of grid cells that contain LAR by the total amount of annotated cells. For the PRAGMA-CF scoring method a minimum intensity projection or slice thickness of maximum 5 mm was used.

Statistical analysis

As our primary aim was to investigate the presence and extent of structural bronchial changes on CT in children with SA, the results are presented as descriptive statistics. Results of the BA analysis are presented from the subsegmental level onward (G_1–G_9), where G_1 represents the subsegmental bronchi. Data are shown as median and interquartile range (IQR) or as mean±SD depending on the data distribution. Multiple CT scans per patient were included in the cross-sectional analysis. We performed sensitivity analysis, including only the first performed CT scan, to investigate whether including multiple scans per patient would significantly affect the prevalence and extent of structural abnormalities. Intra- and interrater reliability testing was performed on 10% of the collected CT scans by two certified and experienced image analysis researchers (WB and QL). Additional information on the methods of reliability testing can be found in the supplementary material. To investigate whether indicators of SAD were related to structural alterations on chest CT we used the mixed-effects modelling framework. We investigated whether patients with $FEF_{25–75\%}$ or $FEF_{75\%}$ z-score < −1.645, the lower limit of normal (LLN) as defined by Global Lung Initiative 2012 [33], had different B_{out}/A, B_{lumen}/A and B_{wt}/A. Besides $FEF_{25–75\%}$ and FEF_{75}%, we also investigated whether patients with FEV_1 and FEV_1/FVC z-scores < −1.645 had different BA ratios. We also studied whether patients with LAR had different B_{out}/A, B_{lumen}/A and B_{wt}/A. We studied this association per generation and for all combined. In the random effects part, we assumed nested random intercepts for generation and individual. In the fixed effects part, we studied the interaction between group (*e.g.* $FEF_{25–75}$ and FEF_{75} <LLN *versus* $FEF_{25–75}$ and FEF_{75} >LLN) and generation on the outcome. We further adjusted for age, sex, height, volume control using a spirometer, ever sensitisation to allergens and inspiratory lung volume in the model. The BA pairs in generation 7–9 were combined into one bin defined as generation 7 (G_7) to increase numbers in these generations. The logarithmic scale for the outcomes was used because some of the assumptions of the residuals were violated. We did not correct for multiple testing, and significance level of 0.05 is assumed.

Results

A flow chart representing the CT collection and image analysis process is shown in figure 1. Patient characteristics are presented in table 1. The intraclass correlation coefficients for the manual semi-quantitative analysis were between 0.58 and 0.97 for the intra-rater and between 0.33 and 0.73 for inter-rater reliability. Details can be found in supplementary table S1. Comorbidities that could potentially have an effect on the current findings can be found in table 1. An overview of CT scan characteristics can be found in supplementary table S2.

Automatic analysis

Inspiratory scans

142 inspiratory scans were analysed using the automatic BA analysis. In total 26 456 bronchi and 20 293 BA pairs were identified. The median bronchus count per CT was 179.5 (135.8–229.3) and the median BA pair count per CT was 144.5 (100–182.8). The BA pair count per generation per CT is shown in supplementary figure S2. B_{lumen}, B_{out} and arterial measurements per generation are shown in supplementary figure S3. Using the cut-off of 1.1 and 1.5 for the B_{out}/A bronchiectasis was observed on 95.8% and 81.7% of the CT scans respectively (figure 3). The median percentage per CT of BA pairs defined as bronchiectasis with an B_{out}/A cut-off ⩾1.1 was 24.6% (12.7–39.3%) and 3.2% (1.1–7.1%) for ⩾1.5 (table 2). The median percentage of BA pairs per CT showing bronchial wall thickening was 41.7% (24.0–79.8%) for B_{wt}/A cut-off of ⩾0.14. Boxplots showing the B_{wa}/B_{oa} per generation can be found in supplementary figure S4.

Expiratory scans

123 expiratory scans were successfully analysed using the LungQ VERA analysis (figure 1). All of the CT scans had LAR observed on them, with a median %LAR of 12.1% (6.6–21.2%) per CT (table 3).

Lung volumes

Lung volumes can be found in supplementary table S3.

Manual analysis

Inspiratory scans

161 inspiratory scans were analysed using the asthma-CT scoring system (figure 1). In contrast to the automated method, bronchiectasis was observed in only 28% and bronchial wall thickening in 88.8% of the chest CT scans using the semi-quantitative scoring method. Full results of this scoring method are

TABLE 1 Patient characteristics

Age at CT years, mean±SD	11.0±3.8
Female sex, n (%)	69 (42.9)
BMI for age, z-score, mean±SD	0.5±1.3
Height for age, z-score, mean±SD	0.1±1.2
Sensitisation to inhaled allergens, n (%)	94 (58.4)
Patients with >1 CT scan, n	22
Inhaled corticosteroid (mean daily dose), n[#]	
Beclometasone extra fine (434.2 µg)	41
Budesonide (1800 µg)	5
Ciclesonide (492.5 µg)	32
Fluticasone proprionate (437.5 µg)	5
Beclometasone/formoterol (478.6 µg)	42
Fluticasone proprionate/salmeterol (550 µg)	30
Other asthma medication, n	
Leukotriene receptor antagonists	75
Omalizumab	2
Patient history and comorbidities reported, n	
α_1 antitrypsin deficiency	1
Allergic rhinitis	5
Allergy to peanuts	1
Alopecia	1
Congenital cystic adenomatoid malformation[¶]	2
Chronic cough	2
Congenital hypothyroidism	1
Diabetes mellitus type 1	1
Eczema	8
Epilepsy	1
Henoch–Schönlein purpura	1
Hypermobility	1
Hypertension	1
Hypogammaglobulinaemia	3
Prematurity (no bronchopulmonary dysplasia)	15
Spherocytosis	1
Thalassaemia	1
Tonsillectomy	3
Tracheomalacia	1
Trisomy 21	1
Ventricular septal defect correction	1
Spirometry	
FVC z-score, mean±SD	−0.1±1.3[+]
FVC % pred, median (IQR)	98.4 (92.3–108.6)
FEV_1 z-score, mean±SD	−1.0±1.6[+]
FEV_1 % pred, median (IQR)	90.2 (74.4–101.3)
$FEF_{25–75}$ z-score, mean±SD	−1.6±1.6[§]
$FEF_{25–75}$ % pred, median (IQR)	65.5 (44.4–91.2)
FEF_{75} z-score, mean±SD	−1.3±−1.2[+]
FEF_{75} % pred, median (IQR)	64.3 (41.4–95.8)

Table shows the patient characteristics at the time of the CT scan (n=161). CT: computed tomography; BMI: body mass index; FVC: forced vital capacity; FEV_1: forced expiratory volume in 1 s; $FEF_{25–75}$: forced expiratory flow between 25% and 75% of vital capacity; FEF_{75}: forced expiratory flow at 75% of vital capacity. [#]: seven patients no data on medication, one patient with two types of inhaled corticosteroids; [¶]: this diagnosis was made after the first CT was performed; [+]: spirometry data of FVC, FEV_1, FEF_{75} of 10 patients is missing; [§]: spirometry data of $FEF_{25–75}$ of 18 patients is missing.

shown in table 2. Examples of the most frequently observed structural changes can be found in supplementary figure S5.

Expiratory scans

146 expiratory scans were analysed using the PRAGMA-CF scoring method. 82.9% of these CT scans had LAR observed on them, with a median %LAR of 3.3% (IQR 0.7–11.3%) per CT (table 3).

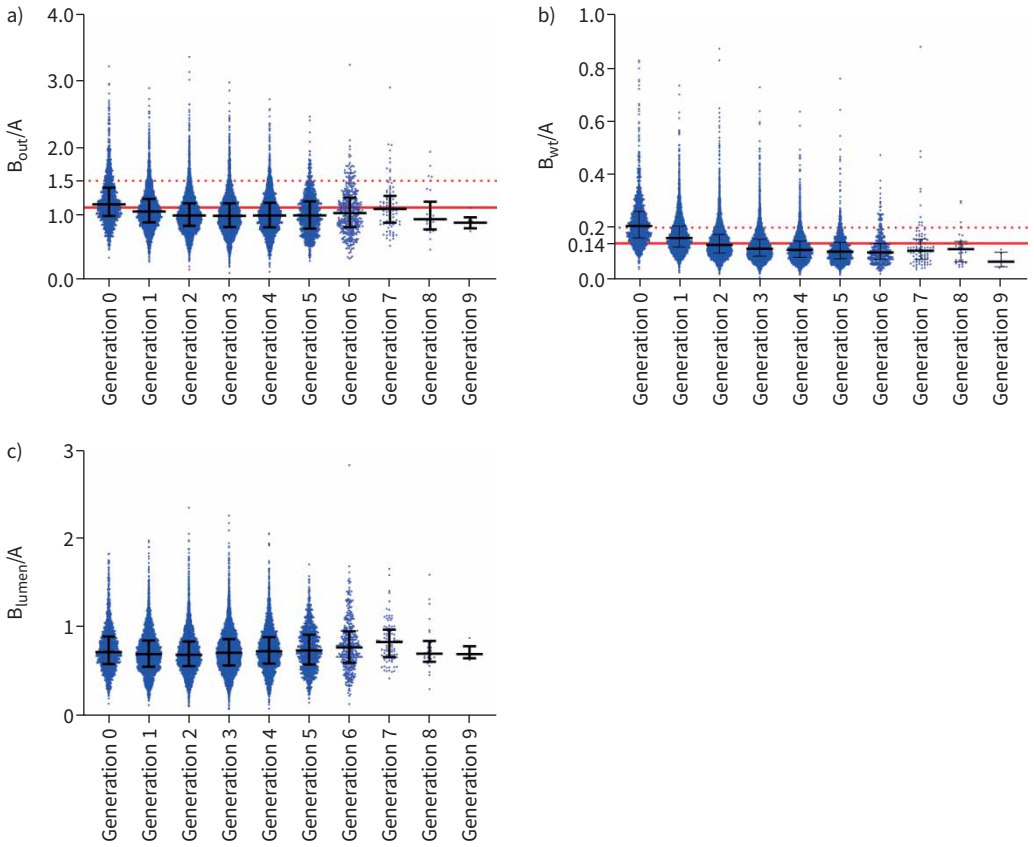

FIGURE 3 Bronchus–artery ratios. This figure shows the B_{out}/A, B_{wt}/A and B_{lumen}/A starting at the segmental level (generation 0). Each blue dot represents an individual bronchus–artery ratio measurement. The black lines indicate the median and interquartile range (25th–75th percentile). a) B_{out}/A per generation: the bold red line indicates the B_{out}/A cut-off of ⩾1.1 and the red dotted line the cut-off of ⩾1.5 for bronchiectasis. b) B_{wt}/A: the bold red line indicates the B_{wt}/A cut-off of 0.14 and the red dotted line the cut-off of ⩾0.20 for bronchial wall thickening. c) B_{lumen}/A per generation. B_{lumen}: bronchial lumen diameter; B_{out}: bronchial outer diameter; B_{wt}: bronchial wall thickness.

TABLE 2 Results of the CT inspiratory analysis

		Automatic BA analysis[#]		Manual analysis[¶]
Bronchiectasis	B_{lumen}/A ⩾0.8	B_{out}/A ⩾1.1	B_{out}/A ⩾1.5	
Bronchiectasis, number of CTs (%)	128 (90.1)	136 (95.8)	116 (81.7)	45 (28)
% Bronchiectasis per CT, median (IQR)	24.0 (5.5–46.1)	24.6 (12.7–39.3)	3.2 (1.1–7.1)	-
Total bronchiectasis score, median (IQR)	-	-	-	2.0 (2.0–4.5)
Bronchial wall thickening		B_{wt}/A ⩾0.14	B_{wt}/A ⩾0.20	
Bronchial wall thickening, number of CTs (%)		142 (100)	138 (97.2)	143 (88.8)
% Bronchial wall thickening per CT, median (IQR)		41.7 (24.0–79.8)	11.1 (4.8–20.3)	-
Total bronchial wall thickening score, median (IQR)		-		4.0 (3.0–6.0)
Other findings				
Mucus plugging, number of CTs (%)		-		52 (32.3)
Total mucus plugging score, median (IQR)		-		1.0 (1.0–2.0)
Atelectasis/consolidation, number of CTs (%)		-		79 (49.1)
Bulla/cysts, number of patients (%)		-		8 (5.0)
Ground glass opacities, number of CTs (%)		-		29 (18)

Table shows the abnormalities that were observed using manual semi-quantitative and automatic image analysis methods. Inspiratory scans were analysed using the fully automatic LungQ software and manually using the asthma-CT scoring method. BA: bronchus–artery; CT: computed tomography; LAR: low attenuation regions. [#]: n=142; [¶]: n=161.

TABLE 3 Results of the CT expiratory analysis

	Automatic VERA analysis[#]	Manual analysis[¶]
Normal lung tissue %, median (IQR)	74.1 (61.8–87.00)	96.7 (88.7–99.3)
LAR %, median (IQR)	12.1 (6.6–21.2)	3.3 (0.7–11.3)
LAR, number of CTs (%)	142 (100)	121 (82.9)
CTs with >5% trapped air, n (%)	100 (81.3)	63 (43.2)

Table shows the abnormalities that were observed using manual semi-quantitative and automatic image analysis methods. Automatic analysis was performed using the "Ventilation Estimation deep learning Analysis" (VERA) software (Thirona B.V.) and PRAGMA-CF for the manual analysis. VERA determines four categories of lung tissue: normal, low attenuation region, emphysema and low attenuation regions with emphysema (only normal lung tissue and low attenuation regions are presented). CT: computed tomography; LAR: low attenuation regions. [#]: n=123; [¶]: n=146.

Associations between BA ratios and SAD

There were respectively 40.4% (55 out of 136) and 46.6% (62 out of 133) patients with a FEF_{75} and $FEF_{25–75}$ z-score < −1.64 (indicating SAD).

FEF_{75} z-score <1.645 (supplementary tables S4–S6)

Patients with FEF_{75} z-scores below the LLN had significantly smaller B_{lumen}/A than patients with FEF_{75} above the LLN (p=0.007). Patients with FEF_{75} z-scores below the LLN had significantly higher B_{wt}/A than patients with FEF_{75} above the LLN (p=0.011). B_{out}/A was not different between the groups with FEF_{75} z-scores >LLN and <LLN (p=0.094). Effects plots are shown in figure 4.

$FEF_{25–75}$ z-score < −1.645 (supplementary tables S7–S9)

Patients with $FEF_{25–75}$ z-scores below the LLN had significantly smaller B_{lumen}/A than patients with $FEF_{25–75}$ above the LLN (p=0.021). Patients with $FEF_{25–75}$ z-scores below the LLN had significantly higher B_{wt}/A than patients with FEF_{75} above the LLN (p=0.023). B_{out}/A was not different between the groups with $FEF_{25–75}$ z-scores >LLN and <LLN (figure 4).

FEV_1 and FEV_1/FVC z-score < −1.645 (supplementary tables S10–S15)

There was no difference in B_{lumen}/A and B_{out}/A between the groups with FEV_1 z-scores >LLN and <LLN. Patients with FEV_1 z-scores below the LLN had significantly higher B_{wt}/A than patients with FEV_1 z-scores above the LLN (p=0.029).

Patients with FEV_1/FVC z-scores below the LLN had significantly smaller B_{lumen}/A than patients with FEV_1/FVC z-scores above LLN (p=0.007). Patients with FEV_1/FVC z-scores below the LLN had significantly higher B_{wt}/A than patients with FEV_1/FVC above the LLN (p=0.005). B_{out}/A was not different between the groups with FEV_1/FVC z-scores >LLN and <LLN.

LAR (automatic and manual) (supplementary tables S16–S21)

Patients with higher %LAR detected by LungQ had significantly smaller B_{lumen}/A than patients with lower %LAR(p=0.007). Patients with higher %LAR had higher B_{wt}/A than patients without LAR (p<0.0001). B_{out}/A were not different between patients with LAR and without LAR (figure 5).

Patients with higher %LAR detected by the PRAGMA-CF scoring method had significantly higher B_{wt}/A than patients with lower %LAR (p<0.0001). B_{lumen}/A and B_{out}/A were not different between patients with LAR and without LAR. The full results of the mixed model analyses can be found in supplementary tables S4–S15).

Discussion

In this study we identified substantial structural bronchial changes in the large and small airways on chest CT scans of children with SA. We observed that almost all CTs, analysed by the automatic BA analysis, showed bronchiectasis and all thickened bronchi. Moreover, we found that lung function indicators of SAD were related to bronchial wall thickening.

The most important and surprising finding was the high prevalence and extent of bronchiectasis on chest CT scans. Other imaging studies found a prevalence for bronchiectasis of 20–30% in children with SA [14, 17], which is similar to the prevalence found by using manual semi-quantitative scoring in our study.

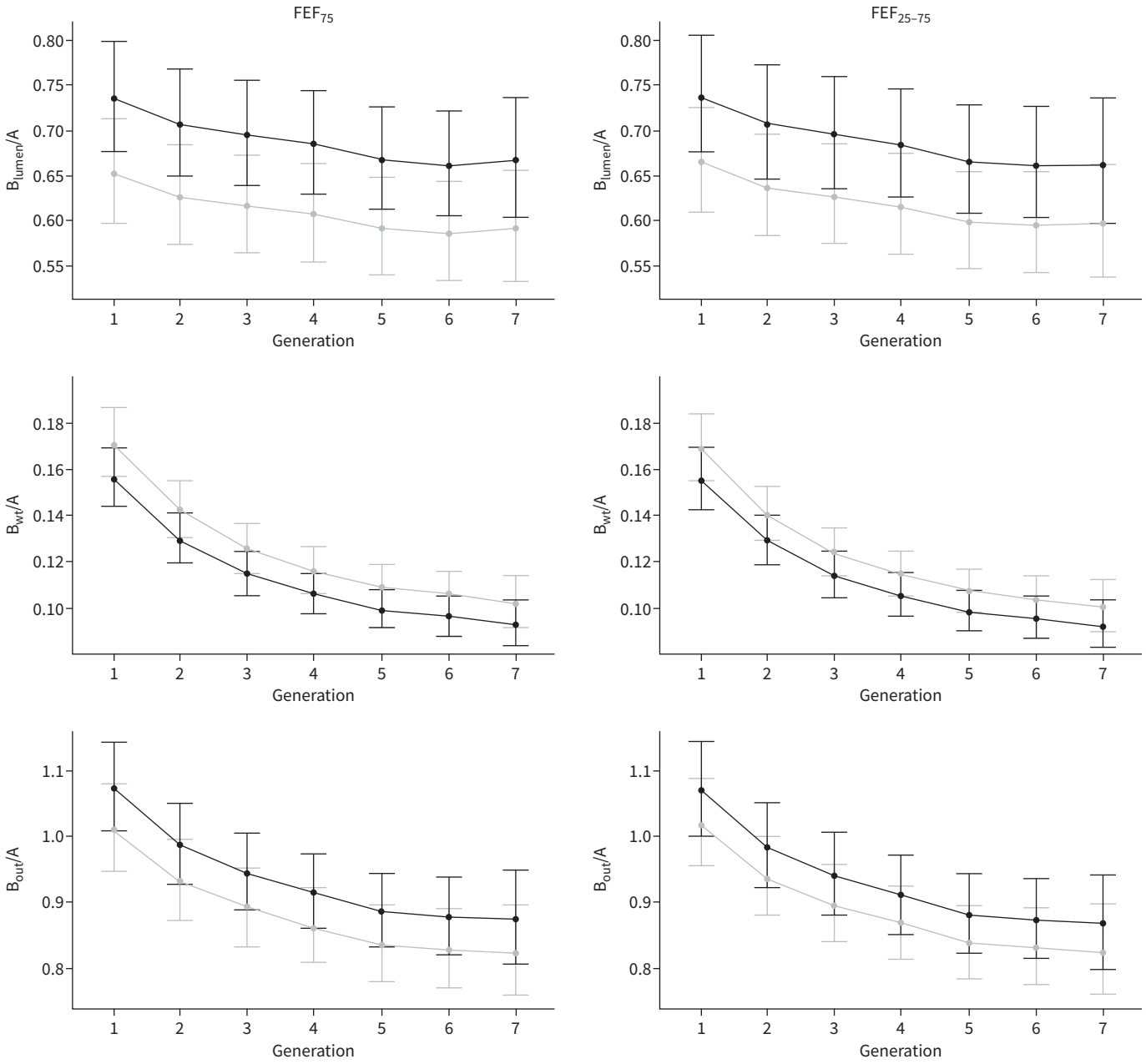

FIGURE 4 Effects plots of the mixed model analysis studying the association between airway–artery ratios and end-expiratory flows. The left-hand graphs show the results of forced expiratory flow at 75% (FEF_{75}) of vital capacity and the right-hand graphs show the results of forced expiratory flow between 25% and 75% ($FEF_{25–75}$) of vital capacity. The grey line indicates a FEF_{75} or $FEF_{25–75}$ z-score< −1.645 and the black line indicates a FEF_{75} or $FEF_{25–75}$ z-score> −1.645. For these plots we assume the mean/mode of all these variables: age, sex, height, spirometer-controlled computed tomography, allergic sensitisation and inspiratory lung volume. For both FEF_{75} and $FEF_{25–75}$ we observed a significant overall difference for B_{lumen}/A and B_{wt}/A, but not for B_{out}/A. Fixed effect estimates and standard errors can be found in the supplementary material. B_{lumen}: bronchial lumen diameter; B_{out}: bronchial outer diameter; B_{wt}: bronchial wall thickness.

However, for the automatic BA analysis we report much higher prevalence and extent of bronchiectasis in children with SA.

This discrepancy in findings can have several reasons. Firstly, previous studies used manual semi-quantitative scoring systems. Manual scoring of bronchiectasis is performed by visually comparing the diameter of the bronchus with the adjacent artery. Although this technique is sensitive to detect severely widened bronchi, it is most likely not sensitive enough to detect more subtle widening of the

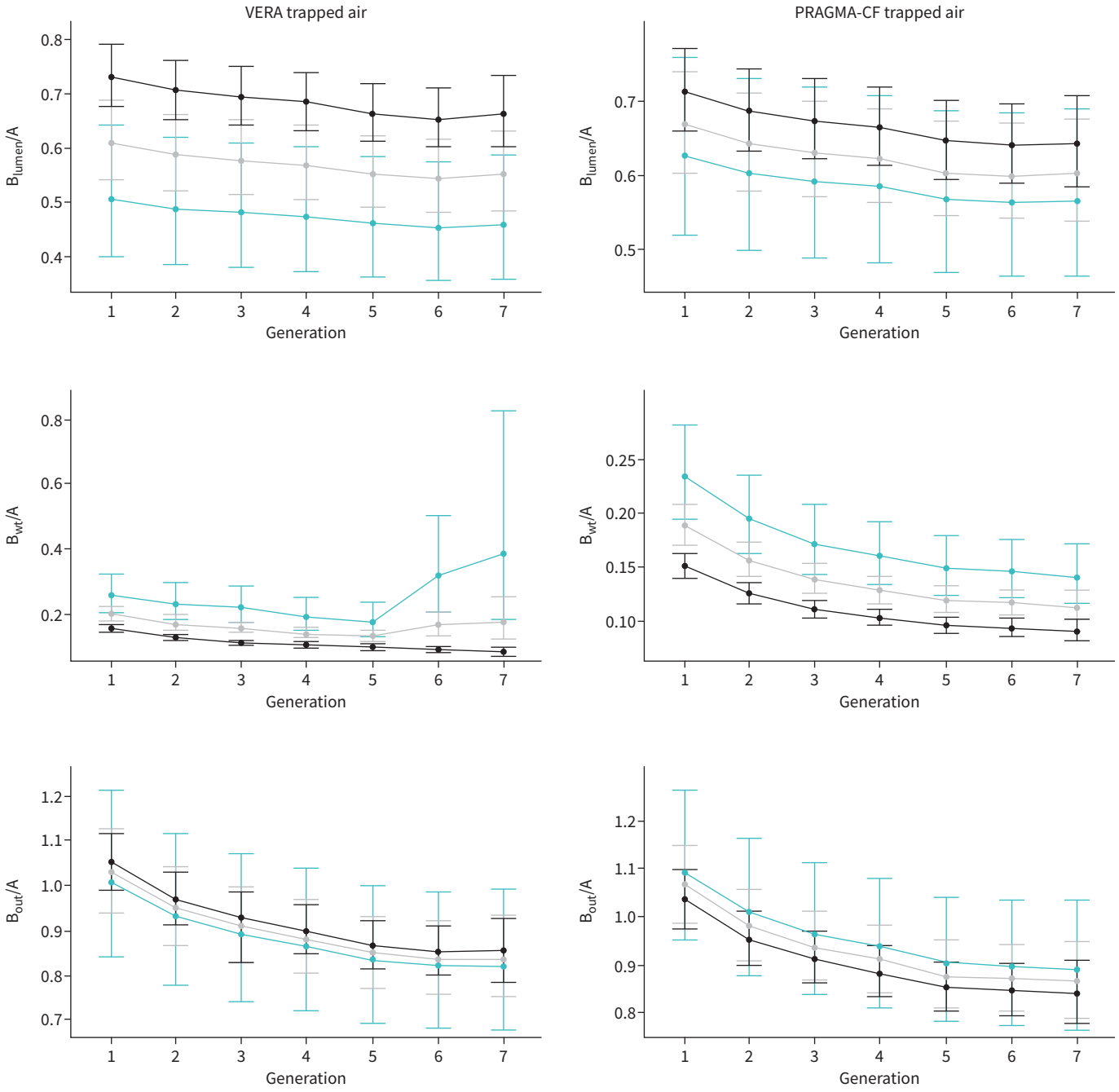

FIGURE 5 Effect plots of the mixed model analysis studying the association between bronchus–artery ratios and low attenuation regions (LAR) measured by the automatic "Ventilation Estimation from Registered Analysis" (VERA) analysis and manual PRAGMA-CF analysis. The left-hand graphs show the results of the VERA analysis, and the right-hand graphs show the results of the PRAGMA-CF analysis. The black line indicates the predicted B_{lumen}/A, AB_{wt}/A and B_{out}/A ratios for 0% LAR (minimum), grey line for 23.51% (half of maximum) and blue for 47.01% (maximum). For these plots we assume the mean/mode of all these variables: age, sex, height, spirometer-controlled CT, allergic sensitisation and inspiratory lung volume. For LAR detected by VERA the model shows us that increased LAR on CT is associated with B_{lumen}/A and B_{wt}/A, but not B_{out}/A. For LAR detected by VERA we observed an interaction between LAR and generation for B_{wt}/A, indicating that B_{wt}/A ratios were different in higher generations for patients with increased LAR. For LAR detected by PRAGMA-CF the model shows us that increased LAR is associated with B_{wt}/A but not B_{lumen}/A and B_{out}/A. B_{lumen}: bronchial lumen diameter; B_{out}: bronchial outer diameter; B_{wt}: bronchial wall thickness.

smaller bronchi in the higher generations. For sensitive detection of bronchiectasis precise measurements of all BA dimensions are needed [19]. The automatic BA analysis enables a large number of BA dimensions to be measured even in higher generations and with greater precision in comparison to manual

semi-quantitative scoring methods used in previous studies. Secondly, it is possible that the spirometry-controlled CT protocol and extensive breathing manoeuvre training by the patient has contributed to a more sensitive detection of abnormal widened bronchi in this study. Volume standardisation results in CT scans at or near TLC, on which higher numbers of BA pairs can be observed relative to CTs acquired at lower lung volumes [27].

For the diagnosis of bronchiectasis we used a B_{out}/A cut-off value of 1.1. In a recent international consensus statement, it was stated that a B_{out}/A of ⩾1.0 was suspect for bronchiectasis [28]. In children the "European Respiratory Society guidelines for the management of children and adolescents with bronchiectasis" advises to use the B_{lumen}/A cut-off of >0.8 [34]. The evidence for the use of this cut-off however is limited. In addition, we believe that the use of the B_{lumen}/A cut-off for the diagnosis of bronchiectasis is less sensitive, because the presence of mucus in a widened airway can reduce the B_{lumen} diameter. Our cut-off of 1.1 was derived from a study in children with CF and control subjects, which were analysed using the same automatic BA analysis as in our study [22]. In addition, the cut-off of 1.1 is close to what has been used in other bronchiectasis studies [28, 29]. In addition to the B_{out}/A cut-off of 1.1, we also used a more conservative B_{out}/A cut-off of 1.5, which has been suggested to define bronchiectasis in adults [28]. Despite this higher cut-off, the prevalence of bronchiectasis was still very high (82%).

Bronchial wall thickening

Besides bronchiectasis we also observed a high prevalence and extent of bronchial wall thickening. Bronchial wall thickening is a well-established remodelling feature of SA which has been observed in multiple imaging studies in children with SA [11, 14–18]. Bronchial wall thickening is suggested to be the result of ongoing remodelling and inflammation [3]. The high percentage of bronchial wall thickening in our study despite intensive standard of treatment is therefore a worrisome observation. Our results conflict with a number of studies where a lower prevalence of bronchial wall thickening was found. The arguments for our high prevalence are similar to the one discussed for the B_{out}/A. Currently, there is no uniformly accepted radiological definition for bronchial wall thickening making it even more difficult to compare findings between studies. To define bronchial wall thickening, we used a B_{wt}/A cut-off of ⩾0.14, which was derived from a study in children with CF and healthy volunteers using the automatic analysis [22]. In addition, we also used a more conservative cut-off of ⩾0.20, which is similar to what has been used in a previous study [30]. Further validation of this cut-off, using the automatic BA analysis, is needed to be able to use it for the diagnosis and evaluation of treatment response.

Small airways disease

In addition to the changes observed in the large bronchi we observed more severe disease in the smaller bronchi as indicated by the higher B_{out}/A and B_{wt}/A (figure 3). Involvement of the small bronchi is further supported by the considerable amount of LAR on the majority of CTs as assessed by PRAGMA-CF on expiratory CTs and by using the VERA analysis. LAR on expiratory scans is considered to be the result of premature closure of the small bronchi during expiration due to inflammation and/or remodelling, resulting in trapped air and/or hypoperfusion [6]. The presence of LAR is therefore considered to be a sensitive indirect indicator of SAD. We observed slightly less LAR than what has been described in another study in children with SA [15]. However, in this study a stringent cut-off of −856 Hounsfield units was used to determine the age of LAR [15]. The use of a stringent cut-off for determining LAR in children might not be as accurate because lung density changes with age, lung volume and positioning of the patient in the supine position (anterior *versus* posterior) [27, 35]. Tracking the density change of a specific voxel from a CT scan at inspiration to that same voxel taken from the CT scan at expiration using the VERA analysis might be a more sensitive method to assess the presence and quantify the extent of SAD. The increased sensitivity of this automatic VERA analysis may also explain why the extent of SAD as assessed using VERA is higher compared to LAR as assessed by PRAGMA-CF (supplementary figure S1).

The importance of the small airways in SA in our study is further supported by the association between reduced end-expiratory flows and BA dimensions. Higher B_{wt}/A were observed for subjects with reduced FEF_{75} and $FEF_{25–75}$. In addition, decreased B_{lumen}/A were observed for subjects with decreased FEF_{75} and $FEF_{25–75}$. These findings support the use of end-expiratory flows as indicators of SAD. In addition, %LAR was also associated with a decrease in B_{lumen}/A and increase in B_{wt}/A.

Limitations

This study has some limitations. The first and most important limitation is the lack of an age-matched control group in this study to validate our findings. To mitigate this limitation we used well-established cut-off values for bronchiectasis [28]. The criterion that is most frequently used to define bronchiectasis in

the literature is an BA ratio of 1.0 or higher [29]. We chose to use the B_{out}/A cut-off value of 1.1 as this was considered to be the optimal threshold to differentiate between normal bronchi and bronchiectasis in children with CF and normal controls using manual BA measurements. The main problem of using these cut-off values is that they are based on manual annotations and not automated measurements. In this study, we assumed that cut-off values determined manually are also valid for automated measurements. As a healthy control group is lacking in this study, the upper limit of normal for the automated BA measurements is unknown. This could explain why there is a large disparity in prevalence and extent of bronchiectasis and bronchial wall thickening between the automated and manual method. Preliminary analysis of a large cohort of chest CTs from patients that underwent CT for a non-pulmonary indication ("Normal Chest CT study Group") with the automatic bronchus–artery analysis show that the current cut-off values may well match the upper limit of normal in this "Normal Chest CT Study Group" (unpublished observations) [36].

The second limitation is related to the retrospective design. One of the consequences of this design was that different CT scanners and scanning protocols were used. This might have somewhat reduced our sensitivity to detect structural changes. Furthermore, not all the CTs could be analysed automatically as they did not meet the technical requirements for the software. By using the retrospective design, however, we were able to include a relatively large group of CTs compared to previous studies in children with SA that ranged from 19 to 88 study subjects [11, 14–18]. Owing to the retrospective design of this study, it is unclear in what percentage of the SA patients that visited our tertiary care outpatient clinic chest CT scans are performed. It is therefore unclear to what extent our results are generalisable for the larger SA population. Clearly, multicentre studies are needed using harmonised CT protocols, image analysis methods and indications for performing a chest CT to further investigate the prevalence and extent of remodelling in SA.

A third limitation is that most SA patients were on treatment with long-acting β agonists at the time of CT. The use of bronchodilators prior to the CT scan might have contributed to the observed bronchial widening in this study. A fourth limitation is related to the use of the artery as reference structure for bronchial size. The use of the artery as reference is based on the assumption that in healthy subjects bronchi and their adjacent artery are similar in size. Currently, it is unknown to what extent BA ratios are affected by changes in arterial diameters as a result of (severe) asthma. In a small autopsy study in patients with fatal asthma and non-smoking non-asthmatic controls no differences in arterial size were observed [37]. In another study in adults with SA the pulmonary vasculature was studied using CT. In this study they found that the combined volume of pulmonary arteries and veins was decreased in patients with SA in comparison to healthy controls [38]. However, in contrast to the other study arterial diameters were not investigated in this study. Whether arterial dimensions in children with SA are normal needs to be further investigated. Bronchial wall thickening might theoretically result in hypoventilated regions leading to local hypoxic pulmonary vasoconstriction with a decrease of arterial diameter as a result, and to an increase of diameters of upstream larger arteries. A decrease in arterial dimensions will result in higher BA ratios, and an increase in arterial dimensions in lower BA ratios. To overcome this limitation, it is of great importance that reference values of bronchi and pulmonary arteries in healthy individuals are developed. In addition, for the diagnosis of bronchiectasis automated detection of tapering needs to be developed, this allows the bronchi to be evaluated independently of the arteries [39]. Despite this limitation, we believe that the observed widening and thickening of the bronchi are the main reason for the increased ratios because of their associations with functional measurements. Finally, we included a relative "old" cohort of SA patients, as there were only two patients on omalizumab prior to the CT. This might not reflect the current SA population.

Clinical implications

Our study suggests that extensive structural bronchial changes are present in children with SA, which is in line with observations in other studies [11, 14–18]. The high extent of bronchiectasis observed with the automatic analysis, however, is new and raises the question whether the pathophysiology of SA and bronchiectasis are interrelated. Furthermore, it raises the question why the treatment for these children with SA was not able to prevent or reverse bronchiectasis [40]. Unfortunately, our study is not able to answer this question because of the retrospective design and the small number of patients with longitudinal CT scans. In general, bronchiectasis in adults is considered to be irreversible [28]. We therefore think it is unlikely that bronchi showing B_{out}/A $\geqslant$1.5 can reverse to normal. However, a small study performed in children with asthma showed that bronchial dilatation ("inner bronchial diameter greater than adjacent artery") could be reversible [40]. Whether more subtle bronchial dilatation (B_{out}/A $\geqslant$1.1) is reversible with appropriate treatment remains to be investigated in longitudinal studies. In our population few patients were on biologics at the time of CT acquisition. Thus, we believe that it might be relevant to investigate whether the use of biologics may have a positive effect on the prevalence and extent of these structural airway

changes. Intervention studies in SA evaluating newer biologicals should consider chest CT as outcome to measure the impact of these biologics on structural bronchial changes. Besides using CT as an outcome measure in clinical trials, we feel that chest CT should be included in the standard workup of SA, as the presence of bronchiectasis will have implications for the further diagnostic workup and management of these patients [41].

Automatic measurement of bronchus–artery dimensions may further aid in the early detection of bronchial abnormalities as it is not affected by the high interobserver variability that is associated with manual annotation. However, before automatic measurements can be used, it is of great importantance that the currently well-established cut-off values are validated for this technique.

In conclusion, we have shown that substantial structural bronchial changes are present in SA. Most CT scans showed a large extent of bronchiectasis and bronchial wall thickening. Structural changes were more severe in patients with reduced end-expiratory flows and LAR. Our findings support the use of chest CT in the workup of SA. Finally, inclusion of chest CT outcome measures should be considered in clinical trials investigating potential disease-modifying therapies for SA.

Provenance: Submitted article, peer reviewed.

Acknowledgement: The authors thank R. Wichertjes (Erasmus MC–Sophia Children's Hospital, Rotterdam, the Netherlands) for preparing all the scans and M. Kemner (Erasmus MC–Sophia Children's Hospital, Rotterdam, the Netherlands) for data support.

Author contributions: W.B. van den Bosch initiated the study; contributed to the design of the work, data collection and analyses; and drafted the manuscript to the final version. Q. Lv contributed to data collection and analyses, and gave final approval to the manuscript. E-R. Andrinopoulou contributed to the analyses and gave final approval to the manuscript. M.W.H. Pijnenburg contributed to the design of the work and gave final approval to the manuscript. P. Ciet contributed to the design of the work and gave final approval to the manuscript. H.M. Janssens contributed to the design and analyses of the work, and gave final approval to the manuscript. H.A.W.M. Tiddens initiated the study, contributed to the design of the work and data analyses, and drafted and gave final approval to the manuscript.

Conflict of interest: W.B. van den Bosch reports an unconditional research grant for a PhD from Vectura Group PLC during the conduct of the study (contract was signed in 2018 for the duration of 4 years). Q. Lv and E-R. Andrinopoulou have nothing to disclose. M.W.H. Pijnenburg reports support from Sanofi and Novartis outside the submitted work. P. Ciet reports personal fees from Vertex, Chiesi Pharmaceuticals BV and Editamed SRL, and grants from the Dutch Research Council, outside the submitted work. H.M. Janssens reports grants and other support from Vertex Pharmaceuticals outside the submitted work. H.A.W.M. Tiddens reports personal fees from Thirona BV during the conduct of the study; and grants and other support from Novartis, personal fees from Vertex and Insmed, and grants from Vectura Group PLC, outside the submitted work. In addition, H.A.W.M. Tiddens has a patent for the PRAGMA-CF scoring system licensed and Sophia Research BV of the Erasmus MC–Sophia Children's Hospital has, in the past 3 years received unconditional research grants from Novartis and Vectura Group PLC, research grants from IMI, CFF, ECFS and the Sophia Foundation, and honoraria and travel expenses for lectures and participation on expert panels from Novartis, Insmed and Vertex. He heads the Erasmus MC core laboratory LungAnalysis which is a not-for-profit core image analysis laboratory. The financial aspects of the laboratory are handled by Erasmus MC.

References

1 Pijnenburg MW, Fleming L. Advances in understanding and reducing the burden of severe asthma in children. *Lancet Respir Med* 2020; 8: 1032–1044.
2 Kaminsky DA, Chapman DG. Asthma and lung mechanics. *Compr Physiol* 2020; 10: 975–1007.
3 King GG, James A, Harkness L, *et al.* Pathophysiology of severe asthma: we've only just started. *Respirology* 2018; 23: 262–271.
4 Wilson SJ, Rigden HM, Ward JA, *et al.* The relationship between eosinophilia and airway remodelling in mild asthma. *Clin Exp Allergy* 2013; 43: 1342–1350.
5 Crimi C, Ferri S, Campisi R, *et al.* The link between asthma and bronchiectasis: state of the art. *Respiration* 2020; 99: 463–476.
6 King GG, Farrow CE, Chapman DG. Dismantling the pathophysiology of asthma using imaging. *Eur Respir Rev* 2019; 28: 180111.
7 van den Bosch WB, James AL, Tiddens HAWM. Structure and function of small airways in asthma patients revisited. *Eur Respir Rev* 2021; 30: 200186.

8 Lipworth B, Manoharan A, Anderson W. Unlocking the quiet zone: the small airway asthma phenotype. *Lancet Respir Med* 2014; 2: 497–506.
9 O'Reilly R, Ullmann N, Irving S, *et al.* Increased airway smooth muscle in preschool wheezers who have asthma at school age. *J Allergy Clin Immunol* 2013: 131: 1024–1032, 1032e1021–1016.
10 Saglani S, Payne DN, Zhu J, *et al.* Early detection of airway wall remodeling and eosinophilic inflammation in preschool wheezers. *Am J Respir Crit Care Med* 2007; 176: 858–864.
11 de Blic J, Tillie-Leblond I, Emond S, *et al.* High-resolution computed tomography scan and airway remodeling in children with severe asthma. *J Allergy Clin Immunol* 2005; 116: 750–754.
12 Tiddens HAWM, Kuo W, van Straten M, *et al.* Paediatric lung imaging: the times they are a-changin'. *Eur Respir Rev* 2018; 27: 170097.
13 Chung KF, Wenzel SE, Brozek JL, *et al.* International ERS/ATS guidelines on definition, evaluation and treatment of severe asthma. *Eur Respir J* 2014; 43: 343–373.
14 Lo D, Maniyar A, Gupta S, *et al.* High prevalence of bronchiectasis on chest CT in a selected cohort of children with severe Asthma. *BMC Pulm Med* 2019; 19: 136.
15 Silva T, Zanon M, Altmayer S, *et al.* High-resolution CT pulmonary findings in children with severe asthma. *J Pediatr (Rio J)* 2021; 97: 37–43.
16 Saglani S, Papaioannou G, Khoo L, *et al.* Can HRCT be used as a marker of airway remodelling in children with difficult asthma? *Respir Res* 2006; 7: 46.
17 Roach DJ, Ruangnapa K, Fleck RJ, *et al.* Structural lung abnormalities on computed tomography correlate with asthma inflammation in bronchoscopic alveolar lavage fluid. *J Asthma* 2020; 57: 968–979.
18 Marchac V, Emond S, Mamou-Mani T, *et al.* Thoracic CT in pediatric patients with difficult-to-treat asthma. *AJR Am J Roentgenol* 2002; 179: 1245–1252.
19 Kuo W, de Bruijne M, Petersen J, *et al.* Diagnosis of bronchiectasis and airway wall thickening in children with cystic fibrosis: objective airway-artery quantification. *Eur Radiol* 2017; 27: 4680–4689.
20 Perez-Rovira A, Kuo W, Petersen J, *et al.* Automatic airway-artery analysis on lung CT to quantify airway wall thickening and bronchiectasis. *Med Phys* 2016; 43: 5736.
21 Weikert T, Friebe L, Wilder-Smith A, *et al.* Automated quantification of airway wall thickness on chest CT using retina U-Nets: performance evaluation and application to a large cohort of chest CTs of COPD patients. *Eur J Radiol* 2022; 155: 110460.
22 Lv Q, Gallardo-Estrella L, Andrinopoulou ER, *et al.* Automatic analysis of bronchus-artery dimensions to diagnose and monitor airways disease in cystic fibrosis. *Thorax* 2023; in press [https://doi.org/10.1136/thorax-2023-220021].
23 Chen Y, Lv Q, Andrinopoulou ER, *et al.* Automatic bronchus and artery analysis on chest computed tomography to evaluate the effect of inhaled hypertonic saline in children aged 3-6 years with cystic fibrosis in a randomized clinical trial. *J Cyst Fibros* 2023; in press [https://doi.org/10.1016/j.jcf.2023.05.013].
24 Global Initiative for Asthma (GINA). Difficult-to-Treat and Severe Asthma in Adolescents and Adult Patients, Diagnosis and Management. 2019. Available from: http://ginasthma.org/
25 Scott AM, Kolstoe S, Ploem MC, *et al.* Exempting low-risk health and medical research from ethics reviews: comparing Australia, the United Kingdom, the United States and the Netherlands. *Health Res Policy Syst* 2020; 18: 11.
26 Cooper BG, Stocks J, Hall GL, *et al.* The Global Lung Function Initiative (GLI) Network: bringing the world's respiratory reference values together. *Breathe (Sheff)* 2017; 13: e56–e64.
27 Salamon E, Lever S, Kuo W, *et al.* Spirometer guided chest imaging in children: it is worth the effort! *Pediatr Pulmonol* 2017; 52: 48–56.
28 Aliberti S, Goeminne PC, O'Donnell AE, *et al.* Criteria and definitions for the radiological and clinical diagnosis of bronchiectasis in adults for use in clinical trials: international consensus recommendations. *Lancet Respir Med* 2022; 10: 298–306.
29 Meerburg JJ, Veerman GDM, Aliberti S, *et al.* Diagnosis and quantification of bronchiectasis using computed tomography or magnetic resonance imaging: a systematic review. *Respir Med* 2020; 170: 105954.
30 Kuo W, Soffers T, Andrinopoulou ER, *et al.* Quantitative assessment of airway dimensions in young children with cystic fibrosis lung disease using chest computed tomography. *Pediatr Pulmonol* 2017; 52: 1414–1423.
31 Tepper LA, Caudri D, Utens EM, *et al.* Tracking CF disease progression with CT and respiratory symptoms in a cohort of children aged 6–19 years. *Pediatr Pulmonol* 2014; 49: 1182–1189.
32 Rosenow T, Oudraad MC, Murray CP, *et al.* PRAGMA-CF. A quantitative structural lung disease computed tomography outcome in young children with cystic fibrosis. *Am J Respir Crit Care Med* 2015; 191: 1158–1165.
33 Quanjer PH, Stanojevic S, Cole TJ, *et al.* Multi-ethnic reference values for spirometry for the 3–95-yr age range: the global lung function 2012 equations. *Eur Respir J* 2012; 40: 1324–1343.
34 Chang AB, Fortescue R, Grimwood K, *et al.* European Respiratory Society guidelines for the management of children and adolescents with bronchiectasis. *Eur Respir J* 2021; 58: 2002990.
35 Long FR, Williams RS, Castile RG. Inspiratory and expiratory CT lung density in infants and young children. *Pediatr Radiol* 2005; 35: 677–683.

36 Lv Q, Chen Y, Andrinopoulou ER, *et al.* Fully automatic quantitative analysis of airway-artery dimensions and ratios of normal chest CT scans from infancy into adulthood. American Thoracic Society Conference Washington, 2023.

37 Saetta M, Di Stefano A, Rosina C, *et al.* Quantitative structural analysis of peripheral airways and arteries in sudden fatal asthma. *Am Rev Respir Dis* 1991; 143: 138–143.

38 Ash SY, Rahaghi FN, Come CE, *et al.* Pruning of the pulmonary vasculature in asthma. The severe Asthma Research Program (SARP) cohort. *Am J Respir Crit Care Med* 2018; 198: 39–50.

39 Kuo W, Perez-Rovira A, Tiddens H, *et al.* Airway tapering: an objective image biomarker for bronchiectasis. *Eur Radiol* 2020; 30: 2703–2711.

40 Gaillard EA, Carty H, Heaf D, *et al.* Reversible bronchial dilatation in children: comparison of serial high-resolution computer tomography scans of the lungs. *Eur J Radiol* 2003; 47: 215–220.

41 Chang AB, Boyd J, Bush A, *et al.* International consensus statement on quality standards for managing children/adolescents with bronchiectasis from the ERS CRC Child-BEAR-Net. *Eur Respir J* 2022; 59: 2200264.